Picosecond band filling in highly excited In-Ga-As-P films

J. M. Wiesenfeld and A. J. Taylor*
AT&T Bell Laboratories, Crawford Hill Laboratory, P.O. Box 400, Holmdel, New Jersey 07733
(Received 4 April 1986; revised manuscript received 20 August 1986)

The dynamics of dense electron-hole plasmas in submicrometer-thick In-Ga-As-P films, subsequent to photoexcitation by a 0.5-ps optical pulse, are studied by measuring time-resolved changes in the absorbance of the films at an energy 1 eV above the band gap. Initial electron-hole pair densities are between 6.5×10^{18} and 1.0×10^{20} cm^{-3}. Extensive band filling is observed as a partial bleaching of absorption at the probe wavelength. The bleaching scales in magnitude with the initial photoexcited carrier density, and is due to a plasma which has a temperature between 300 and 600 K, at a delay after photoexcitation of 0.5—1 ps. The bleaching decays into an induced absorption, due to instantaneous band-gap renormalization, in a time that decreases from 20 ps at 1.0×10^{20} carriers/cm^3 to $\sim$5 ps at 6.5×10^{18} carriers/cm^3. However, the initial decay time of the bleaching, 2.8 ± 0.7 ps, is independent of the initial excitation density. The initial decay process could be due to either carrier cooling or plasma expansion. Radiative or Auger band-to-band recombination, or capture by surface or bulk traps, cannot explain the initial decay process of the bleaching.

I. INTRODUCTION

Much of the technology for optical fiber communication systems is based on the In-Ga-As-P alloy system. As the operating speed and level of integration for In-Ga-As-P—based devices increase, it becomes increasingly important to understand the carrier dynamics in this material for ultrashort time scales and ultrasmall distances. There have been some measurements of carrier decay due to Auger recombination,[1-7] and of carrier cooling[8,9] in these materials. In most of these studies[1,2,5-9] moderate initial carrier densities ($<10^{19}$ carriers/cm^3) were created by photoexcitation. In this work, the dynamics of a dense electron-hole plasma (up to 1×10^{20} carriers/cm^3) in In-Ga-As-P is examined by studying changes in absorption that occur on the picosecond time scale.

A dense electron-hole plasma in a semiconductor requires interpretation in terms of many-body theory.[10] Carrier-carrier interactions become prominant. Carrier-lattice interactions, present at low densities, may be altered at high densities. The high-density region of the electron-hole plasma is of particular interest for In-Ga-As-P, since Auger recombination, which occurs at high density, is implicated in the temperature dependence of injection laser threshold in this material.[11] Furthermore, the properties of the high-density electron-hole plasma underlie the operation of optically pumped ultrashort cavity In-Ga-As-P film lasers.[12]

Many effects occur in a dense electron-hole plasma following excitation by an intense ultrashort optical pulse. The band gap is renormalized due to many-body exchange and correlation effects of the dense plasma, with no measurable time delay.[13,14] The initial electron and hole states produced by optical excitation are depopulated by momentum scattering processes within 30—50 fs.[15] The electron and hole populations establish Fermi-Dirac distributions about 0.1—0.3 ps after excitation[14,16] at a temperature higher than the lattice temperature. Carrier cooling starts immediately and continues for times up to $\sim$100 ps after excitation.[17] Simultaneously with all the above processes, the carriers are recombining and the plasma may be expanding spatially.[18-21]

In this study of In-Ga-As-P, the time resolution is 0.5 ps, so that the carriers are assumed to have already established Fermi-Dirac distributions at the earliest time of observation. The optical excitation produces a density of carriers that is much higher than the background (unintentional) doping level, so that the electron and hole densities (n and p, respectively) are equal. We see evidence for extensive bandfilling that persists for up to about 10 ps after excitation at an energy about 1 eV above the band gap. The decay kinetics of the absorption changes due to the dense electron-hole plasma are not consistent with radiative or Auger recombination, and may be due to carrier cooling[17] or to a rapid spatial expansion of the dense plasma.[18-21]

II. EXPERIMENTAL SECTION

Films of In-Ga-As-P are photoexcited by 2 nJ, 0.5 ps pulses at 0.625 μm from a cavity-dumped, passively modelocked cw ring dye laser. Changes in transmission and reflection were measured simultaneously using a probe pulse, which is a time-delayed replica of the pump pulse, with 0.1 nJ energy. The pump and probe beams were parallel, but not collinear, and were focused to a common Gaussian spot of 12 μm diameter, as determined by transmission through a calibrated pinhole. The reflected probe beam propagated collinearly and counter to the incoming pump beam, and was separated from the pump using a 2% reflecting beam splitter. Consequently, the reflected probe beam was weak, and the measured changes in reflectivity have poorer signal-to-noise ratios than the measured transmission changes. The pump beam was chopped and changes in transmission and reflection were measured using phase-sensitive electronics. The time evo-

lution of the changes were recorded on a multichannel analyzer as a scanning optical delay line produced a relative delay between the pump and probe pulses. The transmitted probe beam was detected with a Si p-i-n photodiode, and the reflected probe beam was detected with a photomultiplier. The probe beam could be polarized parallel or perpendicular to the pump beam. Generally, pulses were dumped at a rate of 200 kHz, although control experiments at 80- and 8-kHz dumping rates showed that results were insensitive to laser pulse rate. The results were also unaffected by attenuating the probe beam by a factor of 2. All experiments were performed at 296 K.

The time origin was established by producing a pulse autocorrelation function using two-photon absorption in GaP as the nonlinear mixing process.[22] In this technique, the two-photon absorption of the probe beam in a thin GaP crystal is modulated by the presence of the strong pump beam. Since the autocorrelation is measured as a reduction in intensity of the probe beam, the experimental geometry is identical to that of the pump and probe experiment performed on the In-Ga-As-P sample. This has an experimental advantage over the second harmonic generation (SHG) method for obtaining an autocorrelation function, since for the SHG measurement, one must realign the optics after the sample to detect the ultraviolet second harmonic beam.

The samples used were films of $In_{0.70}Ga_{0.30}As_{0.66}P_{0.34}$ ($E_g=0.96$ eV, $\lambda_g=1.3$ μm) grown lattice matched to InP by liquid-phase epitaxy. The materials were nominally undoped, with residual carrier densities of 5×10^{16} cm^{-3} or less. Films of thicknesses 0.2 ± 0.02, 0.53 ± 0.05, and 0.6 ± 0.06 μm were used. Free films, obtained by etching the InP with an appropriate stop etch,[12] were mounted between a glass slide and a glass cover slip using epoxy of refractive index 1.53. There were no cap layers and there was a large (19%) reflection at the epoxy-In-Ga-As-P interface.

III. RESULTS

Changes in transmission through the photoexcited sample are due to changes in both internal absorption in the sample and reflection at the interfaces of the sample. Assuming both sample interfaces are equivalent (*vide infra*), the transmitted intensity I_t through a strongly absorbing sample ($\alpha l \gg 1$, where α is the absorption coefficient and l is the sample thickness) is

$$I_t = I_0(1-R)^2 e^{-\alpha l} . \tag{1}$$

I_0 is the incident intensity, $R=I_r/I_0$ is the reflection coefficient, and I_r is the reflected intensity. For small changes in transmitted and reflected beam intensities, ΔI_t and ΔI_r, the change in absorption coefficient, $\Delta\alpha$ is given by

$$\Delta\alpha\, l = -\frac{\Delta I_t}{I_t} - \left[2\frac{R}{1-R}\right]\frac{\Delta I_r}{I_r} . \tag{2}$$

Therefore, in order to determine changes in the absorption coefficient, which can be related to carrier distribution functions, it is necessary to measure changes in both the transmitted and the reflected probe beams. For the In-Ga-As-P—epoxy interface, the factor $2R/(1-R)$ has a value of 0.47, and the second term in Eq. (2) is therefore significant.

Time-resolved changes in transmission and reflection are shown in Fig. 1(a) for a 0.2-μm sample excited with a pulse energy of 0.92 nJ. The probe is polarized perpendicular to the pump. The initial density of photoexcited electron-hole pairs n_0 is

$$n_0 = \frac{1.3}{\pi w^2}\frac{E}{h\nu}(1-R_T)\frac{(1-e^{-\alpha l})}{l} , \tag{3}$$

where E is the energy of the excitation pulse, $h\nu$ is the energy per photon at 0.625 μm, w is the Gaussian beam waist parameter, R_T is the total reflection coefficient including the air-glass-epoxy-In-Ga-As-P interfaces. The absorption coefficient α at 0.625 μm is 7.5×10^4 cm^{-1}.[23] The factor of 1.3 converts the Gaussian initial distribution of carriers to an effective uniform density.[5] In view of ambiguities discussed below, more refined approaches for convolving the transverse spatial distributions of pump and probe beams with the carrier density[24] were not utilized. Equation (3) assumes that every absorbed photon creates an electron-hole pair. This is valid for the present experimental conditions, since there is no evidence for nonlinear absorption of the pump up to the highest intensity available from the dye laser.

The change in intensity of the reflected probe beam shown in Fig. 1(a) has been multiplied by 0.47. The deduced transient changes in absorption coefficient, $\Delta\alpha$, computed according to Eq. (2), are shown in Fig. 1(b). At

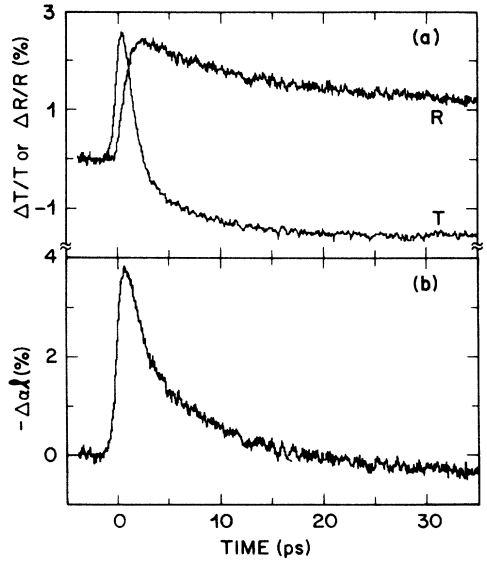

FIG. 1. Time-resolved changes in transmission, reflection, and absorbance for a 0.2-μm-thick film excited to an initial electron-hole pair density of 1×10^{20} cm^{-3}. (a) Transmission and reflection. The changes in reflected beam intensity are multiplied by 0.47. (b) Changes in absorbance, $\Delta\alpha l$. This curve is the sum of the two curves in (a). Bleaching is upward and induced absorption is downward.

early times, $\Delta\alpha < 0$ and the sample shows bleaching. At about 20 ps, the sign of $\Delta\alpha$ changes and the sample shows an induced absorption: $\Delta\alpha > 0$. The induced absorption persists for times longer than 600 ps.[25] Oscillations with a period of 120 ps (for the 0.2-μm thick film) are superimposed on the slowly recovering induced absorption. These are due to coherent acoustic phonons generated in the relaxation of the electron-hole plasma.[25]

For all photoexcited densities, the initial bleaching decays into an induced absorption within 20 ps. The time at which the bleaching is converted to an absorption (i.e., when $\Delta\alpha = 0$) decreases as the initial excitation density decreases, as shown in Fig. 2. The decay of the bleaching (i.e., that part of $\Delta\alpha$ for which $\Delta\alpha < 0$) corresponding to the data of Fig. 2 is shown on a logarithmic scale in Fig. 3. We define a bleaching decay time τ given by $\tau^{-1} = d \ln\Delta\alpha/dt$. The value of τ immediately after excitation is, within experimental uncertainty, the same for all initial densities between 5×10^{18} and 1×10^{20} cm^{-3}. The initial τ has a value of 2.8 ± 0.7 ps. For the highest initial carrier densities, as illustrated in Figs. 2 and 3, there is also a slower component to the decay of bleaching, whose amplitude decreases as excitation density decreases. These results are in contrast to those obtained with excitation at 1.06 μm,[1,2,5,6] in which both the initial decay time of the induced bleaching and the overall decay time of the bleaching increase as the initial carrier density decreases.

For the data shown in Figs. 1–3, the probe is polarized perpendicular to the pump. A comparison of the time-resolved transmission data for parallel and perpendicular relative orientations of the pump and probe beams is shown in Fig. 4(a). For this measurement, the probe is polarized at 45° relative to the pump beam. An analyzer in front of the detector then selects either the parallel or

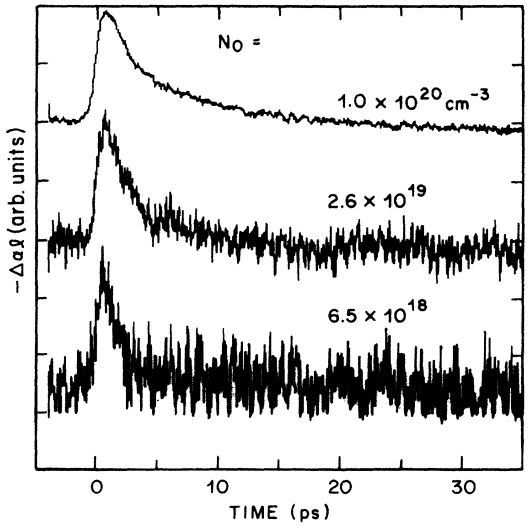

FIG. 2. Time-resolved changes in absorbance for various initial excitation densities, as indicated. Data are for 0.2-μm-thick film (1×10^{20} and 6.5×10^{18} cm^{-3}) and 0.53-μm-thick film (2.6×10^{19} cm^{-3}). The curves are scaled to the same approximate amplitude to facilitate comparison of shapes. Bleaching is upward and induced absorption is downward.

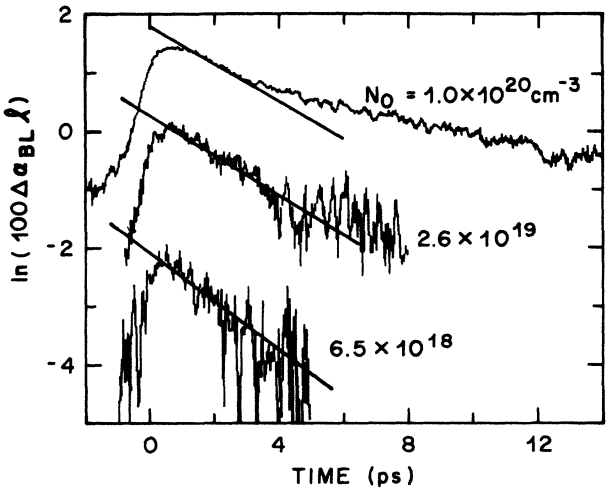

FIG. 3. Semilogarithmic plot of the time-resolved changes in the bleaching for various initial densities. The tangents to the initial decay, as shown, are parallel.

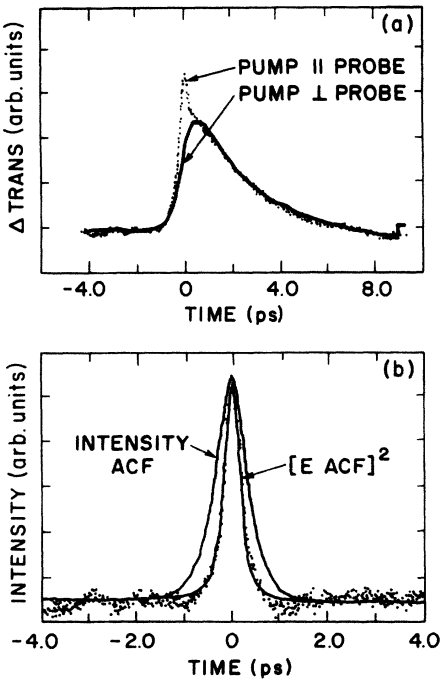

FIG. 4. (a) Comparison of time-resolved transmission changes for parallel and perpendicular relative polarizations of pump and probe beams. The two curves are shown without any relative scaling. The data are for an initial excitation density of 1.8×10^{20} cm^{-3} in the 0.2-μm-thick film. (b) Difference between transmission changes for parallel and perpendicular orientations of pump and probe beams (dots). The difference fits the squared electric field autocorrelation function of the dye laser, $[E\ ACF]^2$, indicating that it is due to coherent coupling between pump and probe. Also shown is the intensity autocorrelation function of the dye laser, which is broader than the coherent coupling contribution.

perpendicular probe component. The curves are identical after 0.5 ps. The peak at $t=0$ for the parallel orientation is due to the coherent coupling contribution.[26] The difference in transmission between parallel and perpendicular orientations is shown on an expanded time scale as the data points in Fig. 4(b). The coherent coupling contribution is identical in shape to the squared electric field autocorrelation function of the dye laser (determined by measurement of its spectrum) as it must be, and is narrower than the intensity autocorrelation function. Furthermore, at $t=0$, the magnitude of the coherent coupling contribution is $53\pm2\%$ of the total signal for the parallel configuration. From these data, we deduce that the perpendicular configuration is free of coherent coupling contribution and that it represents the sample response with a 0.5-ps resolution.

The carrier dynamics are sensitive only to the initially excited density, as given by Eq. (3), and not to the thickness of the film studied. As an example, time-resolved transmission changes that are identical within experimental uncertainty are obtained upon excitation of the 0.2-μm-thick film with 0.60 nJ/pulse and the 0.6-μm film with 1.3 nJ/pulse, as shown in Fig. 5. According to Eq. (3), $n_0=6.5\times10^{19}$ cm^{-3} for both experiments. Other comparisons, including the 0.53-μm film, gave similar results. These results have two implications. (1) The plasma expands so as to uniformly fill the submicrometer thickness of the film in less than 0.5 ps. Thus, use of Eqs. (1) and (3) are justified. (2) Surface effects are not important on the time scale considered here, since the surface site to bulk site ratio changes by a factor of 3 between the 0.2- and 0.6-μm films.

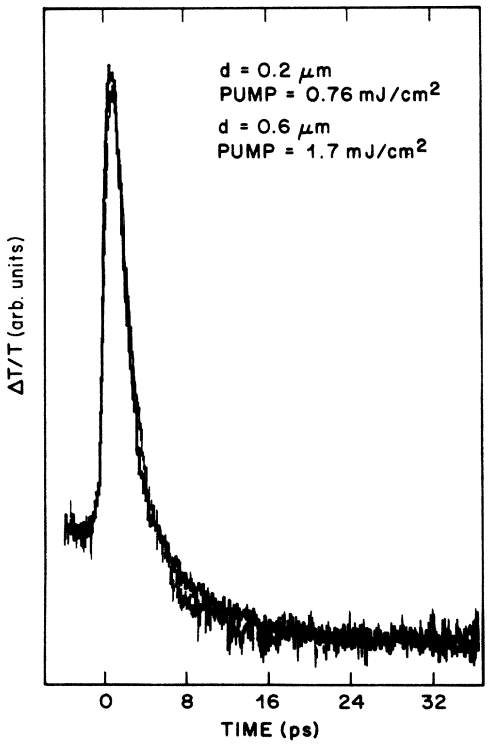

FIG. 5. Time-resolved transmission changes for the 0.2-μm-thick film and the 0.53-μm-thick film, both excited to an initial density of 6.5×10^{19} cm^{-3}.

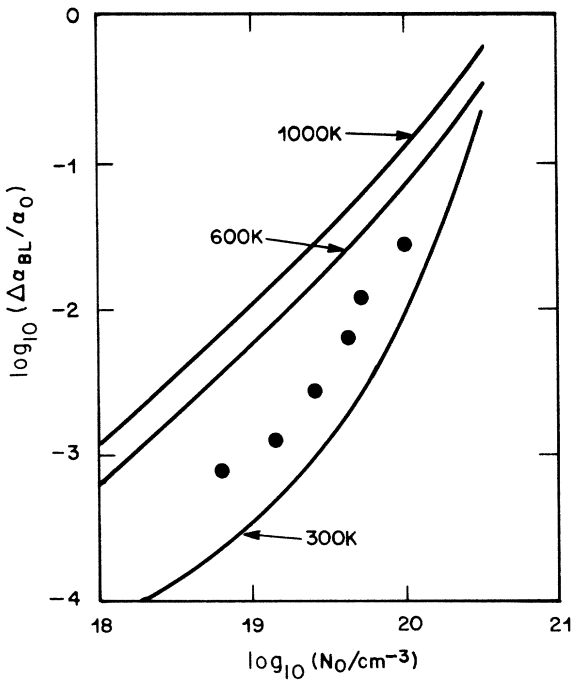

FIG. 6. Peak magnitude of the bleaching relative to the absorption coefficient of the unexcited sample, $\Delta\alpha_{BL}/\alpha_0$, as a function of initial carrier density (points). Calculated bleaching curves are shown for several temperatures.

The peak magnitude of the bleaching is plotted against initial excitation density in Fig. 6. Data are included for films of 0.2 and 0.53 μm thickness. The peak bleaching scales approximately as $n_0^{1.3}$.

IV. DISCUSSION

In these experiments, carriers are created at states far from the edges of the conduction and valence bands, by photons of energy 2 eV. The density of carriers created by photoexcitation far exceeds the residual impurity level in the samples, so the electron and hole concentrations are equal. The probe beam at 2-eV samples states somewhat higher in the bands than the states coupled by initial photoexcitation, due to the reduction of the band gap caused by many-body exchange and correlation effects.[27] The carriers relax to a Fermi-Dirac distribution within 0.3 ps,[14,16] and the states sampled by the 2-eV probe beam reside in the high-energy tails of the distributions in the bands.

In the following sections, we will discuss the bleaching of the sample observed by the probe beam. In Sec. IV A, the peak magnitude of the bleaching is shown to be a consequence of bandfilling. In Sec. IV B, the decay time of the observed bleaching and its mechanistic consequences are discussed.

A. Band filling

The change in absorption coefficient upon excitation of the semiconductor has three components,

$$\Delta\alpha = -\Delta\alpha_{BL} + \Delta\alpha_{BR} + \Delta\alpha_{FC} , \quad (4)$$

where $\Delta\alpha_{BL}$ is the magnitude of bleaching due to change in the distribution of carriers in the conduction and valence bands and $\Delta\alpha_{BR}$ is an increase in band-to-band absorption due to the decrease of band gap because of renormalization. $\Delta\alpha_{FC}$, the free-carrier absorption, is smaller than the other terms and is excluded from further consideration. To proceed further, it is necessary to model the band structure of the material. In-Ga-As-P is a quaternary alloy of III-V band structure.[28] The optical transition interrogated by the probe pulse is assumed to be from the heavy-hole valence band to high above the gap in the conduction band, and the band-to-band absorption coefficient is assumed to scale with photon energy $h\nu$ as $\alpha \sim \varepsilon^{1/2} = (h\nu - E_g + \Delta E_g)^{1/2}$. E_g is the band-gap energy. The band-gap renormalization is given by $\Delta E_g = 2\gamma n^{1/3}$.[27] The relevant terms in Eq. (4) are given by

$$\Delta\alpha_{BL} = \alpha_0(1 + gn^{1/3})(f_e + f_h - f_e f_h) , \quad (5)$$

$$\Delta\alpha_{BR} = \alpha_0 g n^{1/3} , \quad (6)$$

$$g = \gamma/(h\nu - E_g) . \quad (7)$$

The absorption coefficient at the probe wavelength before excitation is α_0, and f_i is the Fermi-Dirac distribution function for carrier i,

$$f_i = \{1 + \exp[(\Delta E_i - \mu_i)/kT]\}^{-1} . \quad (8)$$

The Fermi energy is μ_i and ΔE_i is the excess energy of the probe above the band edge. For the case of a parabolic valence band and a nonparabolic conduction band with nonparabolicity parameter r, the excess energies are

$$\Delta E_h = \varepsilon \left(\frac{1 + r\varepsilon}{1 + \frac{m_h}{m_e} + 2r\varepsilon} \right) , \quad (9)$$

$$\Delta E_e = \varepsilon \left(\frac{1 + r\varepsilon\frac{m_e}{m_h}}{1 + \frac{m_e}{m_h} + 2r\varepsilon\frac{m_e}{m_h}} \right) . \quad (10)$$

m_e and m_h are electron and hole effective masses, respectively, and ε is defined above. Equations (5) and (6) are derived in Appendix A.

Values for $\Delta\alpha$ can be calculated as functions of total electron-hole pair density n and temperature from Eqs. (5)–(10) once the Fermi energies are known. The Fermi energies are calculated numerically using the following band-structure parameters:[29] electron mass in the Γ valley $m_\Gamma = 0.0605 m_0$, electron mass in the L valley $m_L = 0.328 m_0$, nonparabolicity $r = 0.968$ eV^{-1}, $\Gamma - L$ valley separation $= 0.76$ eV, $E_g = 0.96$ eV,[28] and heavy-hole mass $m_h = 0.5 m_0$.[28] The band-gap renormalization constant for In-Ga-As-P is $\gamma = 1.6 \times 10^{-8}$ eV cm.[30] For this simple calculation, the valence band is considered to be a doubly degenerate heavy-hole band.

The results of the calculations for $\Delta\alpha_{BL}$ at three temperature are shown in Fig. 6. The experimental data fit between the curves for 600 and 300 K. The results of the calculations are sensitive in detail, but not in general, to the exact band-structure parameters chosen. As a second model of the band structure, the light-hole band is described as a band parallel to the heavy-hole band but displaced downwardly by an amount $\Delta_1 = 0.25$ eV.[28] The probe then samples transitions to different energies in the conduction band originating from the heavy-hole and light-hole bands. Even with this model, all experimental data points except that at $n_0 = 1 \times 10^{20}$ cm^{-3} fall between the 600- and 300-K curves. For both models, $f_h \gg f_e$, so the bleaching transient observed for a probe energy of 1.98 eV is due to the holes.

We therefore conclude that the observed bleaching is due to bandfilling of a dense plasma between 600 and 300 K. The peak bleaching occurs at a time delay of 1.0 ps at $n_0 = 1 \times 10^{20}$ cm^{-3} and 0.5 ps at 6.5×10^{18} cm^{-3}. The bandfilling model requires that Fermi-Dirac carrier distributions be established within 0.5 ps, but this has recently been shown to occur in Ga-As on a time scale of less than 0.3 ps, for carrier densities of less than 10^{18} cm^{-3}.[14,16] Furthermore, the results in Fig. 6 suggest that the plasma has cooled from a maximum temperature $(h\nu - E_g)$ of 3000–4000 K to less than 600 K in 1 ps. This is not unreasonable, and there are analogous observations of rapid cooling in other experiments. Luminescence experiments in In-Ga-As (Ref. 8) and 1.3-μm In-Ga-As-P (Ref. 9) show plasma temperatures below 300 and 500 K immediately after excitation, within the 10-ps resolution of the experiment. For $Ga_{0.56}In_{0.44}P$, a plasma of density 7×10^{18} cm^{-3} excited to a maximum temperature $(h\nu - E_g)$ of 1700 K has been observed to have cooled, after excitation, to 730 K, within the 10-ps experimental resolution.[31] The extensive bandfilling observed here underlies the operation of ultrashort-cavity In-Ga-As-P film lasers, which, because of the band-filling and ultrashort cavity, can produce picosecond pulses at energies high above the band gap.[12]

B. Decay of bleaching

The initial bleaching decay time has a constant value of $\tau = 2.8 \pm 0.7$ ps over the range of initial carrier densities from 1.0×10^{20} to 6.5×10^{18} cm^{-3}. In order to relate the time dependence of $\Delta\alpha$ to changes of carrier density, we start with Eqs. (5)–(7), with $f_h \gg f_e$, as discussed above. Thus, we consider only absorbance changes due to the distribution of excited holes. Equations (5) and (6) are differentiated with respect to time, requiring the derivatives of df_h/dt [from Eq. (8)] and then $d(\Delta E_h - \mu_h)/dt$. Different approximations to the Fermi integral[32] are used to relate carrier density to the Fermi level in the highly degenerate regime [given by $(\mu_h - E_v)/kT > 0.9$] and the weakly degenerate to nondegenerate regime [given by $(\mu_h - E_v)/kT < 1.3$]. E_v is the energy of the valence-band edge. The algebra is straightforward, but tedious. After numerical substitution in the resulting equations, with $p = 1 \times 10^{20}$ cm^{-3} and $p = 1 \times 10^{19}$ cm^{-3} for the high- and low-density regimes, respectively, one of the terms is found to be at least five times larger than the others. A simplified derivation, considering only this dominant term, is given in Appendix B. At high densities, where the plasma is degenerate,

$$\frac{d\ln\Delta\alpha_{\rm BL}}{dt}=\frac{\hbar^2}{3m_hkT}\left[\frac{3\pi^2}{2}\right]^{2/3}p^{-1/3}\frac{dp}{dt}\ . \tag{11}$$

At lower densities, where the plasma is not degenerate or is only weakly degenerate,

$$\frac{d\ln\Delta\alpha_{\rm BL}}{dt}=\frac{1}{p}\frac{dp}{dt}\ . \tag{12}$$

Equations (11) and (12) are derived without assuming a mechanism for carrier decay. They are expressions relating the experimental observable, $d\ln\Delta\alpha/dt$, to carrier density decay. The experimental invariance (within 25%) of $d\ln\Delta\alpha/dt$ as a function of n_0 ($n_0=p_0$) suggests that at high density, from Eq. (11), $dp/dt\approx p^{1/3}$ and at low density, from Eq. (12), $dp/dt\approx p$.

In order to explain the results, we will consider decay due to traps, band-to-band recombination (radiative and Auger), carrier cooling, and plasma expansion. During the following discussion, the results of a recent study[30] of time-resolved luminescence of In-Ga-As-P films excited by 0.5-ps pulses at 0.625 μm (as in this study), in a spot diameter of 5 or 26 μm, will be utilized. From that study, which had 200-ps resolution, it was found that the luminescence 200 ps after excitation is due to band-to-band recombination by a 300-K plasma of density $\approx 5\times10^{18}$ cm^{-3}, regardless of the initial excitation density over the range from 5×10^{20} to 1×10^{18} cm^{-3}. Furthermore, the intensity of total luminescence 200 ps after excitation increased as the initial excitation density increased, indicating that the majority of carriers were not lost during the first 200 ps. These results suggest that the initial carrier density decay within the first 200 ps after excitation is due to significant plasma expansion, rather than to carrier recombination. After 200 ps, the plasma density decayed due to a combination of Auger and bimolecular radiative recombination, with a $1/e$ decay time of about 2 ns.

The density of bulk traps in In-Ga-As-P grown by liquid-phase epitaxy is less than 5×10^{16} cm^{-3}. This density is insignificant compared to the initially photoexcited density, and would have an effect in the first few picoseconds only if the traps acted as recombination centers with exceedingly short lifetimes. In that case, however, the carrier lifetime would be very short and no band-to-band emission would be observed after 200 ps. Since the films are thin, surface effects could be important. The initial carrier decay time due to surface recombination is

$$\tau=l/2S\ , \tag{13}$$

where S is the surface recombination velocity. For the 0.2 μm thick films, $\tau=3$ ps requires a surface recombination velocity of 3×10^6 cm/sec. This value would be among the largest surface recombination velocities ever reported. Moreover, From Eq. (13), the carrier decay time should be three times larger for the 0.53- and 0.6-μm films, compared to the 0.2-μm film, if surface recombination were the dominant decay mechanism, contrary to the observation. In addition, typical surface recombination velocities for etched surfaces are $\approx$100 cm/sec. Thus, recombination by bulk or surface traps cannot explain the data.

Band-to-band recombination processes also are inconsistent with the data. At low density, the radiative recombination rate is $dp/dt=Bp^2$, where B is the radiative recombination coefficient. Using Eq. (12), this predicts that $d\ln\Delta\alpha/dt\approx p$, contrary to the observation (Fig. 3). The radiative lifetime, τ_r, saturates at a carrier density of about 10^{19} cm^{-3} at 300 K, however, and therefore, at high density, $\tau_r=d\ln p/dt$, is a constant.[5] So far, this is consistent, via Eq. (12), with the experimental observation. However, the saturated value of τ_r is 1 ns,[5] three orders of magnitude slower than the observed bleaching decay time. Thus radiative recombination cannot explain the bleaching decay time.

The data cannot be reconciled with Auger recombination. For Auger recombination, the carrier decay rate is given by

$$\frac{dp}{dt}=Cp^s\ , \tag{14}$$

where C is the Auger recombination coefficient. For low and intermediate densities, $s=3$. At higher densities, the Auger recombination rate can saturate, due to Coulombic screening[33] and/or the consequences of energy and momentum conservation in a degenerate electron-hole plasma.[34] Hence, $s<3$. For In-Ga-As, for example, it has been found that $s=2.16$ for a carrier density above 2.5×10^{18} cm^{-3}, while $s=3$ for lower carrier densities.[6] First consider unsaturated Auger recombination ($s=3$) for In-Ga-As-P. Using the value[5] for the Auger recombination coefficient, $C=2.6\times10^{-29}$ cm^6 sec^{-1} for 1.3-μm In-Ga-As-P, and Eqs. (11) and (14), gives a bleaching decay time of 5 ps, for an electron and hole density of 1×10^{20} cm^{-3}. This value is not far from the observed τ. However, when the Auger rate is unsaturated, dp/dt will change markedly with p. Therefore, according to Eq. (11), the bleaching decay time would be expected to vary markedly with p, in contradiction to the observation. Next, consider a saturated Auger process ($s<3$). For the combination of Eqs. (11) and (14) (assuming a high density for saturation) to yield a bleaching decay time independent of p would require $s=\frac{1}{3}$, which by comparison to the In-Ga-As data,[6] for example, is physically unreasonable. Furthermore, saturation would occur at some density p_S much lower than 1×10^{20} cm^{-3}. Equation (14) would be valid for $p<p_S$, with $C=2.6\times10^{-29}$ cm^6 sec^{-1}, as above. Since $p_S\ll1\times10^{20}$ cm^{-3}, the bleaching decay time [from Eqs. (11) or (12) and (14)] at the value p_S would be much longer than 5 ps. At densities higher than p_S, the bleaching decay time would not decrease (since $s=\frac{1}{3}$), and hence, by this hypothesis, τ is much larger than 5 ps. This contradicts the experimental observation. Thus, the initial bleaching decay time of 2.8 ps cannot be explained by Auger recombination.

Carrier cooling could provide an explanation for the time-dependent data. The variation of $\Delta\alpha_{\rm BL}$ with temperature is obtained by differentiation of Eq. (5) with respect to temperature. After some algebra, the results, maintaining only the largest term, are given by Eq. (15) for the high-density degenerate regime,

$$\frac{d\ln\Delta\alpha_{\mathrm{BL}}}{dt}=\frac{1}{T}\left[\frac{\Delta E_h-\mu_h}{kT}\right]\frac{dT}{dt}\,, \tag{15}$$

and Eq. (16) for the lower density, nondegenerate regime,

$$\frac{d\ln\Delta\alpha_{\mathrm{BL}}}{dt}=\frac{1}{T}\left[\frac{\Delta E_h}{kT}-\frac{3}{2}\right]\frac{dT}{dt}\,. \tag{16}$$

A simplified derivation of Eqs. (15) and (16) is given in Appendix C. To a crude level of approximation, $\Delta E_h>\mu_h$ and $\Delta E_h/kT>\frac{3}{2}$, so Eqs. (14) and (15) become identical. ΔE_h varies little with carrier density. The temperature of the plasma at the time of peak bleaching (0.5—1 ps) is not a strong function of carrier density (Fig. 6), and is approximately 450 K. The experimentally observed constant initial value of $d\ln\Delta\alpha_{\mathrm{BL}}/dt$ would therefore be explained by a carrier-density independent cooling rate dT/dt of about 30 K/ps (or more precisely a constant value of $T^{-2}dT/dt$).

It is quite possible that dT/dt is constant over the range of carrier densities studied here. Screening of the carrier-polar optical-phonon interaction[33,35] and nonequilibrium phonon populations[36,37] have been proposed to explain the decrease in carrier cooling rates in GaAs as the carrier density is increased to the 10^{18}-cm^{-3} level. However, in In-Ga-As-P, hole-nonpolar optical-phonon coupling may be a significant channel for carrier cooling,[9] and since this is short ranged it might not be screened at the highest densities studied here. While there is a reduction in carrier cooling rate as the density is increased from 1×10^{17} to 5×10^{17} cm^{-3} in In-Ga-As-P,[9] it is possible that this reduction is due to the effects of nonequilibrium polar optical-phonon populations, which causes the carrier-polar optical-phonon interaction to be turned off at the densities studied here. The residual cooling rate is due to nonpolar phonon scattering, which would not be very density dependent. Thus, the cooling rate in the high-density regime studied here could be independent of carrier density. Qualitatively, it is therefore possible that the decay of bleaching we observe in In-Ga-As-P is due to cooling of the plasma at an almost carrier independent rate.

Plasma expansion is also a possible explanation for the rapid decay of bleaching. The mathematical formalism for plasma expansion is complex even in one dimension.[18] For simple radial diffusion (which is not plasma expansion, but may have similarities), the decay of carrier density, at $t=0$, sampled by a probe beam of finite diameter will not depend on carrier density, and so would be consistent with a constant value for $d\ln\Delta\alpha/dt$. Moreover, the results of the luminescence experiments on In-Ga-As-P (*vide supra*) provide evidence that plasma expansion, to a final density around $5-6\times10^{18}$ cm^{-3}, has occurred within the 200-ps time resolution of the luminescence experiments.[30] Therefore, the decay of bleaching in the transient absorption experiments could be due to rapid decay of carrier density (but not carrier number) by spatial expansion of the plasma in two dimensions. (Recall the plasma has filled the submicrometer thickness of the film in less than 0.5 ps.) Plasma expansion could also provide an explanation for the second, slower component to the decay of bleaching (Figs. 2 and 3). The slower component observed in the decay of $\Delta\alpha$ at the highest densities might occur because the plasma must expand a greater distance in order to reach a critical plasma density of approximately 5×10^{18} cm^{-3}. At lower densities, the spatial expansion of the plasma would be smaller when the density of 5×10^{18} cm^{-3} is reached, and the expansion might be completed in a shorter time. The decay of $\Delta\alpha_{\mathrm{BL}}$ is completed in about 20 ps for an initial density of 1×10^{20} cm^{-3}. If this corresponds to expansion to a final density of 5×10^{18} cm^{-3} without loss of carriers, the plasma area has expanded 20 times, requiring an increase in diameter from 12 to 50 μm. The radius has increased at a rate of $\approx1\times10^{8}$ cm/sec. This expansion velocity is comparable to the Fermi velocity. In GaAs, plasma expansion at a rate of 10^{7} cm/sec has been suggested.[38] In contrast, plasma expansion in the II-VI compounds CdS and CdSe appears to occur with a "slow drift" velocity of $\approx1\times10^{6}$ cm/sec.[21,39] The carrier profile, which is initially Gaussian due to the pump profile, will evolve into another functional form due to plasma expansion. Because of this, no attempt to convolve the probe profile with a plasma spatial distribution[24] was attempted in this work.

In contrast to the results reported here, other experimental studies of high-density ($\approx10^{19}$ cm^{-3}) excitation in In-Ga-As-P and In-Ga-As have shown evidence for carrier decay due to Auger recombination.[1-6] Due to the longer wavelength excitation in those experiments (1.06 μm or longer), carrier densities as high as 1×10^{20} cm^{-3} were not attainable. The high carrier densities and the small spot size used in the present experiment are both favorable to significant plasma expansion, so it is possible that the present experimental conditions favor plasma expansion at the expense of Auger recombination. Indeed, the luminescence experiments[30] described above show that significant expansion of the plasma has occurred in less than 200 ps. If the initial decay of bleaching is due to carrier cooling, the dynamics of the plasma after cooling will not be measurable with a 1.98-eV energy probe. In that case, the plasma could decay by Auger recombination on a time scale of 10's to 100's of picoseconds without being observed in the present experiment.

Thus far, the induced absorption due to the band-gap renormalization, $\Delta\alpha_{\mathrm{BR}}$ in Eqs. (4) and (6), has not been considered. Due to reduction of the band gap in a high-density plasma, the probe pulse will interrogate states higher in the band after excitation than before excitation. This causes an increase in the background band-to-band absorption at the probe energy after creation of the dense electron-hole plasma, and is probably responsible for the approximately 0.1—0.4% increase in absorption 40 ps after excitation. Equation (6) significantly overestimates $\Delta\alpha_{\mathrm{BR}}$, however, giving a value of 7% at 1×10^{20} cm^{-3} and 3% at 6×10^{18} cm^{-3}. Equation (6) is based on a model assuming parabolic bands which is certainly not valid at the probe energy used. For a nonparabolic conduction band, the magnitude of $\Delta\alpha_{\mathrm{BR}}$ would be reduced, since the density of states for a nonparabolic band is less than that for a parabolic band. It is difficult to see how use of a nonparabolic band structure could reduce $\Delta\alpha_{\mathrm{BR}}$ by a factor of 10, however. Thus, the cause of the small

magnitude of the experimentally observed induced absorption is not clear. Because of this, we have considered $\Delta\alpha_{BL}$ separately from $\Delta\alpha_{BR}$ in the preceding analyses, and will not consider $\Delta\alpha_{BR}$ in more detail.

V. SUMMARY AND CONCLUSIONS

Significant bandfilling occurs in In-Ga-As-P subsequent to creation of a carrier density in the range 6×10^{18} to 1×10^{20} cm^{-3} by photoexcitation with a 0.5-ps pulse. The bandfilling is observed as a bleaching, at early time, of absorption at a probe energy 1 eV above the bandgap. The bleaching decays into an induced absorption (due to band-gap renormalization) about 20 ps after photoexcitation for an initial carrier density of 1×10^{20} cm^{-3}. At lower initial carrier densities, the bleaching decays into an induced absorption more rapidly. However, the initial decay rate of the bleaching, $d\ln\Delta\alpha_{BL}/dt$, is the same for all photoexcited densities between 6×10^{18} and 1×10^{20} cm^{-3}. Band-to-band recombination processes, either radiative or Auger, and capture by traps are excluded as possible mechanisms for the decay of bleaching. The decay of bleaching could be due to carrier cooling or plasma expansion. The present experiment cannot distinguish between these two possibilities. Pump and probe experiments performed with longer wavelength probe pulses would be helpful in further elucidating the decay mechanism of the initial bleaching, as well as in studying the subsequent dynamics of dense electron-hole plasmas in In-Ga-As-P.

ACKNOWLEDGMENTS

We thank J. Stone, A. G. Dentai, and J. F. Ferguson for supplying the In-Ga-As-P samples used in this work. We are grateful to J. Shah for helpful discussions.

APPENDIX A

In this appendix, Eqs. (5) and (6) are derived. In general, the band-to-band absorption coefficient, at a photon energy $h\nu$, is, for a direct-gap semiconductor with parabolic bands,

$$\alpha(h\nu,E_g')=A(h\nu-E_g')^{1/2}(1-f_h)(1-f_e)\ , \tag{A1}$$

where A is a constant containing the matrix elements, etc. The band gap E_g' is density dependent, and is renormalized by an amount[27]

$$\Delta E_g=2\gamma n^{1/3} \tag{A2}$$

so that $E_g'=E_g-\Delta E_g$. Before excitation, $f_h=f_e=0$, the band gap is E_g, and the absorption coefficient is

$$\alpha_0=A(h\nu-E_g)^{1/2}\ . \tag{A3}$$

The change in absorption coefficient at a constant photon energy, due to a Fermi-Dirac distribution of electrons and holes, is therefore

$$\Delta\alpha=A(h\nu-E_g+\Delta E_g)^{1/2}(1-f_h)(1-f_e) - A(h\nu-E_g)^{1/2}\ . \tag{A4}$$

Equation (A4) is rearranged to give

$$\Delta\alpha=\alpha_0\left[1+\frac{\Delta E_g}{h\nu-E_g}\right]^{1/2}(1-f_e-f_h+f_ef_h)-\alpha_0\ . \tag{A5}$$

Define $g=\gamma/(h\nu-E_g)$, as in Eq. (7). Recognizing for the present experiment that $\Delta E_g\ll(h\nu-E_g)$, the square root in Eq. (A5) may be expanded. Using Eq. (A2), the result is

$$\Delta\alpha=-\alpha_0(1+gn^{1/3})(f_e+f_h-f_ef_h)+\alpha_0gn^{1/3}\ . \tag{A6}$$

Equations (5) and (6) follow from Eq. (A6), identifying the first term as $-\Delta\alpha_{BL}$, and the second term as $\Delta\alpha_{BR}$.

APPENDIX B

In this appendix, Eqs. (11) and (12) are derived. For the conditions relevant to the present experiment, $f_h\gg f_e$, and $gn^{1/3}\ll1$, so the dominant contribution to the bleaching can be written as

$$\Delta\alpha=\alpha_0f_h\ . \tag{B1}$$

(For simplicity, we will drop the BL subscript in this appendix.) Taking the time derivative of Eq. (B1), we have

$$\frac{d\,\Delta\alpha}{dt}=-\frac{\alpha_0f_h^2}{kT}\exp[(\Delta E_h-\mu_h)/kT]\frac{d(\Delta E_h-\mu_h)}{dt}\ , \tag{B2}$$

where we have used Eq. (8) for f_h. The energy ΔE_h, from Eq. (9), varies very weakly with time (only through the time variation of ΔE_g), and we will neglect it. Using this, and Eq. (B1) gives

$$\frac{1}{\Delta\alpha}\frac{d\,\Delta\alpha}{dt}=\frac{d\ln\Delta\alpha}{dt}=\frac{f_h}{kT}\exp[(\Delta E_h-\mu_h)/kT]\frac{d\mu_h}{dt}\ . \tag{B3}$$

Since $\Delta E_h>\mu_h$, it follows from Eq. (8) that

$$f_h\exp[(\Delta E_h-\mu_h)/kt]\approx1\ .$$

Therefore,

$$\frac{d\ln\Delta\alpha}{dt}=\frac{1}{kT}\frac{d\mu_h}{dt}\ . \tag{B4}$$

The problem reduces to calculating the density dependence of μ_h. The hole density and μ_h are related by the Fermi integral $F_{1/2}(\eta)$, where $\eta=(\mu_h-E_v)/kT$, and E_v is the valence-band edge (taken to be the zero of energy), according to[32]

$$p=2N_vF_{1/2}(\eta)\ . \tag{B5}$$

N_v is the valence-band effective density of states, and is given by

$$N_v=2\left[\frac{m_hkT}{2\pi\hbar^2}\right]^{3/2}\ . \tag{B6}$$

The factor of 2 in Eq. (B5) is due to the fact that there are two valence bands (light hole and heavy hole, which are assumed degenerate; see discussion in Sec. IV A above), which have a common Fermi level. For In-Ga-As-P with $m_h=0.5m_0$, $N_v=7.5\times10^{18}$ cm^{-3} at 450 K.

To continue analytically, it is necessary to use an ap-

proximation for $F_{1/2}(\eta)$. First consider the high-density regime, for which $\eta > 0.9$. In this range, the approximation for $F_{1/2}(\eta)$ is[32]

$$F_{1/2}(\eta) = \left[\frac{4}{3\pi^{1/2}}\right](\eta^2+1.7)^{3/4} . \tag{B7}$$

Since $E_v = 0$,

$$\mu_h = kT\eta . \tag{B8}$$

From Eqs. (B5), (B7), and (B8), one may calculate $d\mu_h/dt$, with the result

$$\frac{d\mu_h}{dt} = \frac{2kT}{3}\left[\frac{3\pi^{1/2}}{8N_v}\right]^{2/3} \times \left[1-1.7\left[\frac{8N_v}{3\pi^{1/2}p}\right]^{4/3}\right]^{-1/2} p^{-1/3}\frac{dp}{dt} . \tag{B9}$$

For $p = 1\times 10^{20}$ cm^{-3}, the second term in the brackets in Eq. (B9) has a value of 0.02, and can be neglected. Finally, using Eq. (B6) for N_v, and substituting $d\mu_h/dt$ from Eq. (B9) into Eq. (B4), one obtains Eq. (11) for $d\ln\Delta\alpha/dt$ in the high-density regime.

At low and intermediate density ($\eta < 1.3$), the following approximation is used for $F_{1/2}(\eta)$:[32]

$$F_{1/2}(\eta) = \frac{\exp(\eta)}{1+0.27\exp(\eta)} . \tag{B10}$$

Using Eqs. (B5), (B8), and (B10) one finds for μ_h,

$$\mu_h = kT\ln\left[\frac{p}{2N_v-0.27p}\right] . \tag{B11}$$

Differentiating Eq. (B11),

$$\frac{d\mu_h}{dt} = kT\left[\frac{1}{p}\frac{dp}{dt} - \frac{0.27}{2N_v-0.27p}\frac{dp}{dt}\right] . \tag{B12}$$

For $p < 1\times 10^{19}$ cm^{-3}, the second term in Eq. (B12) has a value at least 10 times smaller than that of the first term, and can be neglected. Substitution of Eq. (B12) into Eq. (B4) yields Eq. (12).

In the derivation of Eqs. (11) and (12) outlined above, we have started with the largest term in Eq. (5). It is possible (and more tedious) to keep all terms in Eq. (5), and perform all the appropriate differentiation, to relate $d\ln\Delta\alpha/dt$ to dp/dt and dn/dt. Numerical substitution in the final result for both the high- and low-density regimes, however, shows that the dominant terms in the final expressions, by at least a factor of 5, are those obtained by starting with Eq. (B1).

APPENDIX C

Equations (15) and (16) are derived in this appendix. The dominant term in Eq. (5) is that given in Eq. (B1),

$$\Delta\alpha = -\alpha_0 f_h . \tag{C1}$$

(In this appendix, the subscript BL is omitted.) Assume that the change in $\Delta\alpha$ is due to the variation of f_h with temperature. Then

$$\frac{d\Delta\alpha}{dt} = -\alpha_0\frac{df_h}{dT}\frac{dT}{dt} . \tag{C2}$$

We obtain df_h/dT from Eq. (8). Substitution into Eq. (C2) gives

$$\frac{d\Delta\alpha}{dt} = -\alpha_0 f_h^2\exp[(\Delta E_h-\mu_h)/kT] \times\left[\frac{\Delta E_h-\mu_h}{kT^2}+\frac{1}{kT}\frac{d\mu_h}{dT}\right]\frac{dT}{dt} . \tag{C3}$$

Recalling from Appendix B that

$$f_h\exp[(\Delta E_h-\mu_h)/kT] \approx 1 ,$$

and using Eq. (C1), Eq. (C3) reduces to

$$\frac{1}{\Delta\alpha}\frac{d\Delta\alpha}{dt} = \frac{d\ln\Delta\alpha}{dt} = \left[\frac{\Delta E_h-\mu_h}{kT^2}+\frac{1}{kT}\frac{d\mu_h}{dT}\right]\frac{dT}{dt} . \tag{C4}$$

For the high-density regime, we use Eqs. (B5)–(B8) to relate μ_h to the hole density p. The result is

$$\mu_h = \mu_0\left[1-0.85\left[\frac{kT}{\mu_0}\right]^2\right] , \tag{C5}$$

where μ_0 is the Fermi level for a highly degenerate plasma at $T=0$,

$$\mu_0 = \frac{\hbar^2}{2m_h}\left[\frac{3\pi^2 p}{2}\right]^{2/3} . \tag{C6}$$

Differentiating Eq. (C5) and substituting Eqs. (C5) and (C6) into (C4) gives

$$\frac{d\ln\Delta\alpha}{dt} = \frac{1}{T}\left[\frac{\Delta E_h-\mu_0}{kT}+2.55\left[\frac{kT}{\mu_0}\right]\right] . \tag{C7}$$

For the dense plasma, $kT \ll \mu_0$, the second term of Eq. (C7) can be neglected, and $\mu_h \approx \mu_0$. The result of these approximations in Eq. (C7) gives Eq. (15).

For low-density plasmas, we start with Eq. (B11). From this,

$$\frac{d\mu_h}{dt} = k\ln\left[\frac{p}{2N_v-0.27p}\right] - \frac{2kT}{2N_v-0.27p}\frac{dN_v}{dT} . \tag{C8}$$

In the low-density regime, $2N_v \gg 0.27p$, so

$$\frac{d\mu_h}{dT} = \frac{\mu_h}{T} - \frac{kT}{N_v}\frac{dN_v}{dT} . \tag{C9}$$

From Eq. (B6), $dN_v/dT = (\frac{3}{2})N_v/T$. Hence,

$$\frac{d\mu_h}{dT} = \frac{\mu_h}{T} - \frac{3k}{2} . \tag{C10}$$

Substitution of Eq. (C10) into Eq. (C4) yields Eq. (16).

As in Appendix B, the derivation above has considered only the largest term in Eq. (5). It is possible to include all terms of Eq. (5) and proceed as outlined above. The final results, however, when only the largest terms are kept, will be Eqs. (15) and (16).

*Present address: Los Alamos National Laboratory, University of California, P.O. Box 1663, Los Alamos, NM 87545.
[1]B. Sermage, H. J. Eichler, J. P. Heritage, R. J. Nelson, and N. K. Dutta, Appl. Phys. Lett. **42**, 259 (1983).
[2]E. Wintner and E. P. Ippen, Appl. Phys. Lett. **44**, 999 (1984).
[3]A. Miller, R. J. Manning, A. M. Fox, and J. H. Marsh, Electron. Lett. **20**, 601 (1984).
[4]M. E. Prise, M. R. Taghizadeh, S. D. Smith, and B. S. Wherrett, Appl. Phys. Lett. **45**, 652 (1984).
[5]B. Sermage, J. P. Heritage, and N. K. Dutta, J. Appl. Phys. **57**, 5443 (1985).
[6]B. Sermage, D. S. Chemla, D. Sivco, and A. Y. Cho, IEEE J. Quantum Electron. **QE-22**, 774 (1986).
[7]J. C. V. Mattos, E. O. Gobel, and A. Mozer, Solid State Commun. **55**, 811 (1985).
[8]K. Kash and J. Shah, Appl. Phys. Lett. **45**, 401 (1984).
[9]K. Kash, D. Block, and J. Shah, Phys. Rev. B **33**, 8762 (1986).
[10]C. Klingshern and H. Haug, Phys. Rep. **70**, 315 (1981).
[11]Y. Horikoshi, in *GaInAsP Semiconductor Alloys,* edited by T. P. Pearsall (Wiley, Chichester, 1982), p. 379.
[12]J. M. Wiesenfeld and J. Stone, IEEE J. Quantum Electron. **QE-22**, 119 (1986).
[13]A. Antonetti, D. Hulin, A. Migus, A. Mysrowicz, and L. L. Chase, J. Opt. Soc. Am. B **2**, 1197 (1985).
[14]C. V. Shank, R. L. Fork, R. F. Leheny, and J. Shah, Phys. Rev. Lett. **42**, 112 (1979).
[15]A. J. Taylor, D. J. Erskine, and C. L. Tang, J. Opt. Soc. Am. B **2**, 663 (1985).
[16]J. L. Oudar, D. Hulin, A. Migus, A. Antonetti, and F. Alexandre, Phys. Rev. Lett. **55**, 2074 (1985).
[17]J. Shah and R. F. Leheny, in *Semiconductors Probed by Ultrafast Laser Spectroscopy,* edited by R. R. Alfano (Academic, New York, 1984), Vol. I, p. 45.
[18]M. Combescot, Solid State Commun. **30**, 81 (1979).
[19]J. Modesti, A. Frova, J. L. Staehli, M. Guzzi, and M. Capizzi, Phys. Status Solidi B **108**, 281 (1981).
[20]A. Cornet, T. Amand, M. Pugnet, and M. Brousseau, Solid State Commun. **43**, 147 (1982).
[21]F. A. Majumder, H. E. Swoboda, K. Kempf, and C. Klingshirn, Phys. Rev. B **32**, 2407 (1985).
[22]B. F. Levine, W. T. Tsang, C. G. Bethea, and F. Capasso, Appl. Phys. Lett. **41**, 470 (1982).
[23]H. Burkhard, H. W. Dinges, and E. Kuphal, J. Appl. Phys. **53**, 655 (1982).
[24]E. Wintner, J. Appl. Phys. **57**, 1533 (1985).
[25]J. M. Wiesenfeld, Appl. Phys. Lett. **47**, 143 (1985).
[26]E. P. Ippen and C. V. Shank, in *Ultrashort Light Pulses,* edited by S. L. Shapiro (Springer-Verlag, Berlin, 1978), p. 83.
[27]W. F. Brinkman and T. M. Rice, Phys. Rev. B **7**, 1508 (1973).
[28]T. P. Pearsall, in *GaInAsP Semiconductor Alloys,* edited by T. P. Pearsall (Wiley, Chichester, 1982), p. 295.
[29]M. A. Littlejohn, T. H. Glisson, and J. R. Hauser, in *GaInAsP Semiconductor Alloys,* edited by T. P. Pearsall (Wiley, Chicester, 1982), p. 243.
[30]A. J. Taylor and J. M. Wiesenfeld Phys. Rev. B (to be published).
[31]H. J. Zarrabi and R. R. Alfano, Phys. Rev. B **32**, 3949 (1985).
[32]J. S. Blakemore, *Semiconductor Statistics* (Pergamon, New York, 1962), Appendix C 3.
[33]E. J. Yoffa, Phys. Rev. B **23**, 1909 (1981).
[34]C. Tanguy and M. Combescot, Solid State Commun. **57**, 539 (1986).
[35]R. F. Leheny, J. Shah, R. L. Fork, C. V. Shank, and A. Migus, Solid State Commun. **31**, 809 (1979).
[36]J. Collet, A. Cornet, M. Pugnet, and T. Amand, Solid State Commun. **42**, 883 (1982).
[37]W. Potz and P. Kocevar, Phys. Rev. B **28**, 7040 (1983).
[38]K. H. Romanek, H. Nather, J. Fischer, and E. O. Gobel, J. Lumin. **24-25**, 585 (1981).
[39]H. Saito and E. Gobel, Phys. Rev. B **31**, 2360 (1985).